JOURNAL OF CATALYSIS 56, 453–467 (1979)

Methanation on Supported Nickel Catalysts Using Temperature Programmed Heating

A. E. ZAGLI, J. L. FALCONER, AND C. A. KEENAN

Department of Chemical Engineering, University of Colorado, Boulder, Colorado 80309

Received July 28, 1978; accepted October 14, 1978

The techniques of temperature programmed desorption and temperature programmed reaction were used to study methanation of carbon monoxide on three high-weight loading, supported nickel catalysts. A flow system at atmospheric pressure and a mass spectrometer detector was used to continuously monitor the products leaving the surface. The desorption spectra of adsorbed CO and of CO_2 were dependent on the catalyst properties. On all three catalysts CO and CO_2 desorbed from the surface during heating following CO adsorption. Products were observed leaving the surface up to temperatures in excess of 500°C. The reaction of coadsorbed CO and H_2 as well as the reaction of adsorbed CO with flowing H_2 were studied on each of the catalysts. Both CH_4 and H_2O were observed leaving the catalyst surface at the same temperature indicating that C–O bond breaking was rate determining. The results show that temperature programmed desorption is a very useful technique for studying reaction mechanisms as well as characterizing catalysts.

INTRODUCTION

The techniques of temperature programmed desorption (TPD) and temperature programmed reaction (TPR) were used to study the kinetics and mechanisms of methanation of CO on three supported nickel catalysts. In addition to studying methanation on these catalysts, the desorption properties for carbon monoxide and carbon dioxide were also studied.

Recent work (*1–3*) has indicated a carbide is an intermediate for the methanation reaction and the present reaction studies were carried out to both verify this and obtain additional information. Also, Vannice (*4*) reported that methanation proceeded more rapidly on supported Pt and Pd than on unsupported Pt and Pd. In addition, he found that increasing the acidity of the support resulted in an increase in the methane turnover number. Vannice related this increase in activity to an increase in the surface concentration of the more weakly bound CO species and also found a correlation between specific activity and CO–metal bond strength (*5*). We studied the temperature programmed desorption spectra of CO to see if a similar effect was observed for nickel.

Temperature programmed desorption (TPD), also called flash desorption when used to study desorption from wires and foils in high vacuum, has been applied to supported catalysts to study desorption but it has not been used much to study catalytic reactions. In this paper temperature programmed desorption and temperature programmed reaction (TPR) are used with supported catalysts to provide kinetic information that has not been obtained by other techniques. In particular, the desorp-

0021-9517/79/030453-15$02.00/0

tion properties of the CO and CO_2 are studied as well as the reaction of H_2 with CO. Comparisons between different catalysts can be readily made using these techniques. In differential reactor studies only the activity (or the activation energy and pre-exponential factor) and the order of reaction can be measured on catalysts for comparison. In TPR studies the fraction converted, the shape of the reaction product curve, the peak temperature for that curve, the number of reaction curves, and the shape and temperatures of the unreacted desorbing reactants can all be measured. In addition, the heating rate can be varied to measure activation energies, and the initial surface coverage can be varied to determine the order of reaction. Also, the surface coverage of reactants can be measured. Thus more detailed comparisons can be made between different catalysts and much more kinetic information can be obtained using TPR. In general, an adsorbed gas desorbs in several distinct desorption peaks and TPR can be used to tell which of these corresponding adsorption states are most reactive and which are least reactive. This paper contains initial studies of reactant desorption and methanation studied by temperature programming methods.

The three catalysts chosen for study were all supported nickel. Catalyst A was a commercial methanation catalyst with an alumina support and catalyst C was a commercial hydrogenation catalyst with a kieselguhr support. Catalyst A contained additional ingredients added to prevent sintering. Catalyst B was prepared in a University laboratory as a methanation catalyst and was supported on alumina. In this paper a comparison will be made between these three catalysts to show the large differences that are observed in TPD and TPR studies.

In addition, since the desorption of simple gases, such as CO, has been widely studied using single and polycrystalline foils, these published results will be compared to our results from supported catalysts in an effort to obtain a better understanding of the relationship between the unsupported macrocrystals and the supported microcrystals.

EXPERIMENTAL DETAILS

The temperature programmed desorption apparatus used in these studies was similar to one described in the literature (*6*). The crushed catalyst sample (0.1 to 0.2 g) was placed on a quartz frit contained in a 1-cm-o.d. quartz reactor. The catalyst was heated by a small furnace and 0.07-mm-o.d. chromel-alumel thermocouple wires placed in the catalyst measured its temperature. A temperature programmer was used to control catalyst heating at a linear rate and most experiments reported in this paper used heating rates of 0.8 to 1.5°K sec^{-1}. A carrier gas of helium at atmospheric pressure flowed over the catalyst at 1.7 cm^3 sec^{-1}. This gas stream was sampled through a sampling valve immediately downstream of the catalyst and was analyzed by a Bendix time-of-flight mass spectrometer.

Using a gas-tight syringe, 1-cm^3 aliquots of gas were exposed to the catalyst by injection into the helium stream through a septum located immediately upstream of the catalyst. The mass spectrometer was calibrated by repeated injections of these 1-cm^3 aliquots. All adsorptions were carried out at room temperature to saturation coverage. After allowing the excess gas to be removed by helium flow, the catalyst was heated so as to increase the temperature at a constant rate, and both a mass signal and the thermocouple output were simultaneously recorded. A plot of rate of desorption (or reaction) versus catalyst temperature was then obtained from this data. To avoid complications from cracking in the mass spectrometer ionizer, methane was observed by the mass 15 signal.

Materials

Three supported nickel catalysts were used in this study. Catalyst A was obtained from Girdler Chemical and contained 25.4% nickel, 8% CaO, and 4% C on alumina (G-65 RS). The catalyst as supplied was reduced and stabilized. Catalyst B was prepared by impregnation of alumina with $Ni(NO_3)_2 \cdot 6H_2O$ in Professor Bartholomew's laboratory and contained 15% nickel on alumina. It also was reduced and passivated (*7*). Catalyst C was obtained from Harshaw Chemical Company and contained 55% nickel present as nickel oxide mounted on kieselguhr (Ni 0102 T $\frac{1}{8}$). Metal surface area data were available only for catalyst B. It had a hydrogen uptake of 167 μmoles H_2/g catalyst corresponding to a nickel surface area of 14.6 m^2/g catalyst (dispersion of 13.8%) (*8*).

Each catalyst was crushed and 20–40 mesh particles were used in the quartz reactor. The catalysts were reduced in H_2 for 2 hr at 500°C and cooled in He before use.

Helium carrier gas (Air Products, UPC grade, 99.995%) was purified by passing it through Girdler G-43 platinum on γ-alumina catalyst at 200°C, and then through Lindle molecular sieve (5A) immersed in liquid nitrogen. Hydrogen gas (Air Products, zero grade, 99.997%) was purified by passing it through a Palladium Deoxo purifier (Engelhard) and a molecular sieve immersed in liquid nitrogen. The carbon monoxide (Air Products, UHP grade, 99.8%) was passed through activated carbon (Darco) to adsorb carbonyls before use. The carbon dioxide was Coleman grade (Air Products, 99.99%) and was used without further purification. The methane was UHP grade (Matheson, 99.97%) and was used without further purification.

RESULTS

Both the desorptions of adsorbed CO and CO_2 and the reaction of H_2 with CO to form methane were studied on the three catalysts. Results will be reported for each catalyst separately and a comparison made in the discussion section. At room temperature no methane adsorption was observed on any of the catalysts.

Adsorption and Desorption Studies

Catalyst A. A fresh catalyst sample was reduced in H_2 at 500°C, cooled in He to room temperature and then programmed

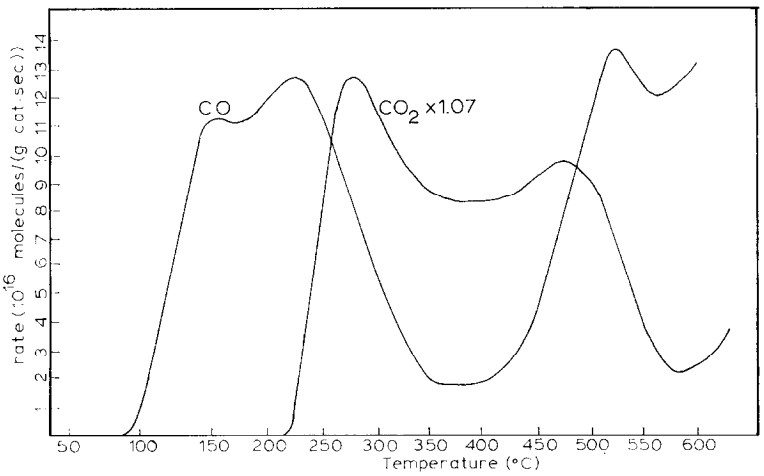

FIG. 1. CO and CO_2 programmed desorption spectra for CO adsorption on catalyst A.

heated to 650°C. Above the reduction temperature, both CO and CO_2 were observed desorbing from the freshly reduced catalyst, with CO_2 desorption occurring at a lower temperature than CO desorption. The heating was stopped at 650°C though the desorption rates had not reached maximums, indicating that much of the CO and CO_2 had not yet desorbed from the surface. Once the catalyst had been heated to 650°C it was not used for any subsequent experiments.

Carbon monoxide adsorbed at room temperature on a freshly reduced catalyst to a saturation coverage of 6.1×10^{19} molecules/g catalyst. The surface coverages measured by the pulse technique with the mass spectrometer were accurate to $\pm 10\%$. As seen in Fig. 1, during subsequent programmed heating both CO and CO_2 were observed desorbing from the surface. The CO desorption had a broad peak(s) near 150°C and a high temperature peak near 550°C. The CO_2 desorption started above 200°C and consisted of several peaks with a high temperature tail. Because of the presence of the high temperature desorption it was difficult to obtain an accurate measure of the amount of CO and CO_2 desorbing from the surface. Approximately 38% of the adsorbed CO desorbed as CO.

Carbon dioxide adsorbed on catalyst A to a saturation coverage of 3.4×10^{19} molecules/g catalyst. Subsequent programmed heating yielded the CO_2 desorption shown in Fig. 2; *no* CO was observed desorbing from the surface below 550°C. When the catalyst was exposed to a pulse of CO_2 gas during adsorption, the CO_2 mass signal downstream of the catalyst very slowly decreased to its initial background level, in contrast to the rapid decrease seen for CO. Such behavior is indicative of slow desorption of weakly bound CO_2, i.e., physically adsorbed CO_2, possibly on the alumina support. To test this possibility the catalyst was oxidized for 2 hr in air at 500°C. On the oxidized surface no CO adsorbed, but 3.3×10^{19} molecules of CO_2/g catalyst adsorbed, and the CO_2 desorption spectra were very similar to those from the reduced surface.

Catalyst B. The desorption properties of catalyst B, which was also nickel on alumina, were quite different from catalyst A. No CO or CO_2 desorption was observed when the freshly reduced catalyst was heated to 650°C. Heating the catalyst after saturation with 8.3×10^{19} molecules

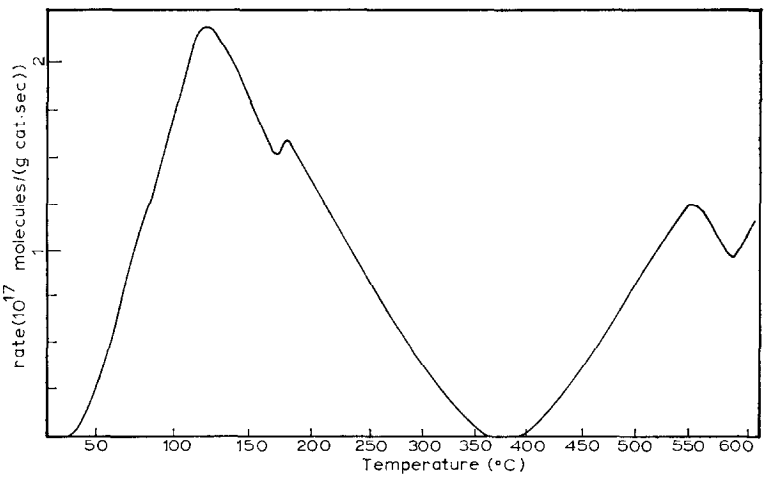

FIG. 2. CO_2 programmed desorption spectrum for CO_2 adsorption on catalyst A.

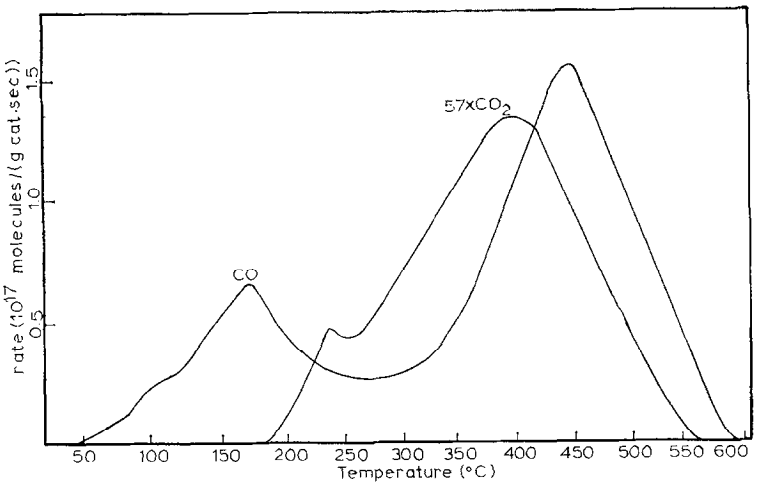

FIG. 3. CO and CO_2 programmed desorption spectra for CO adsorption on catalyst B.

CO/g catalyst yielded the CO and CO_2 desorptions shown in Fig. 3. Because of the absence of high temperature CO and CO_2 peaks it was possible to accurately measure the amount of CO and CO_2 desorption. Only 27% of the adsorbed CO desorbed as CO, with the rest reacting to C and CO_2.

Carbon dioxide adsorbed on this catalyst to a coverage of 3.4×10^{19} molecules/g catalyst, and its desorption, which occurred in two very distinct peaks, is shown in Fig. 4. No carbon monoxide was observed desorbing from the catalyst following CO_2 adsorption.

Bartholomew and Farrauto (7) have measured the H_2 uptake on this catalyst as 2.0×10^{20} H atoms/g catalyst.

Catalyst C. The same desorption experiments were also carried out on catalyst C, the nickel-on-kieselguhr catalyst. Heating the freshly reduced catalyst to 650°C resulted in CO desorption similar to that seen for catalyst A but *no* CO_2 desorption was observed. Figure 5 shows the CO and CO_2 desorption spectra resulting after CO

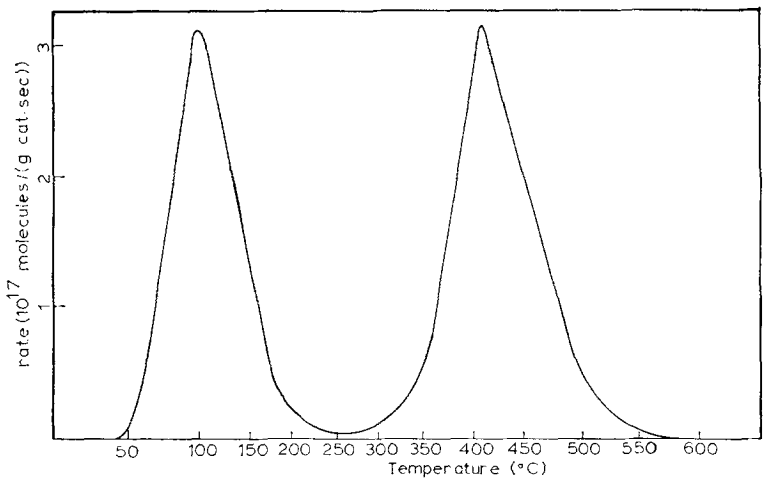

FIG. 4. CO_2 programmed desorption spectrum for CO_2 adsorption on catalyst B.

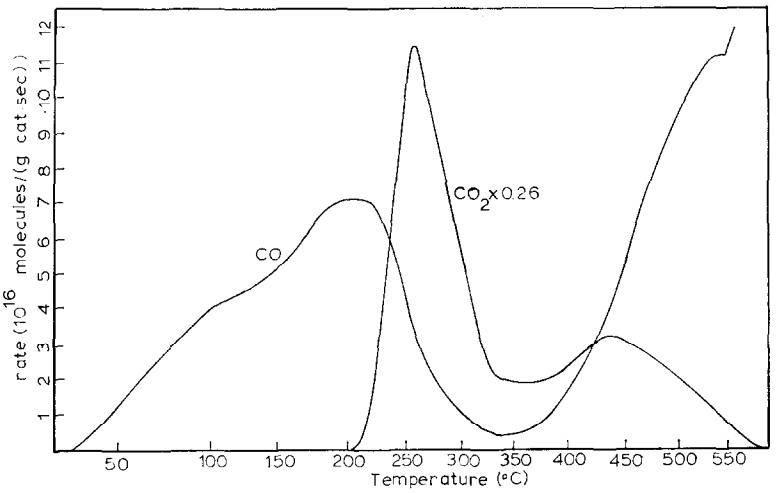

FIG. 5. CO and CO_2 programmed desorption spectra for CO adsorption on catalyst C.

was adsorbed to a saturation coverage of 7.9×10^{19} molecules/g catalyst. Approximately 23% of the adsorbed CO desorbed as CO, the rest decomposing to C and CO_2. On catalyst C, the CO_2 adsorption was much smaller and its desorption spectra will be reported in the near future.

Coadsorption and Reaction Studies

Three types of reaction experiments were performed to study CO hydrogenation to methane. All adsorptions were done at room temperature and during desorption CO, CO_2, CH_4, and H_2O were observed. These three experiments were as follows:

(i) The catalyst, saturated with CO, was exposed to H_2 pulses until no additional H_2 uptake was observed. The catalyst temperature was then increased at a constant rate in the helium carrier gas.

(ii) The catalyst, saturated with H_2, was

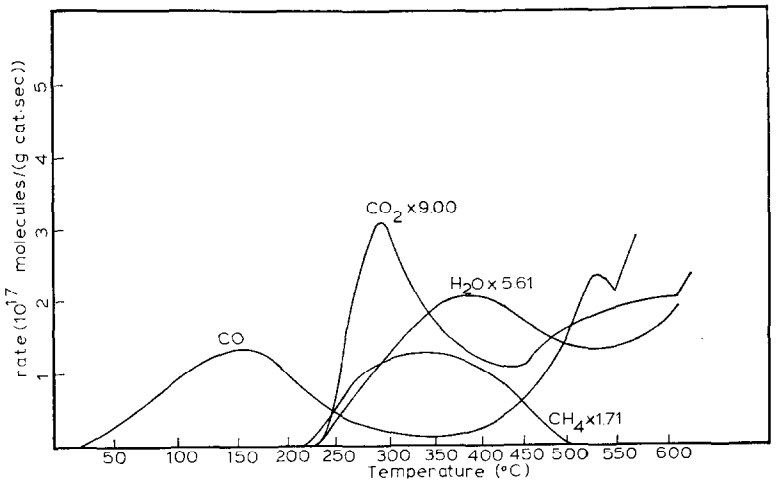

FIG. 6. CO, CO_2, and CH_4 programmed reaction spectra for CO and H_2 coadsorption on catalyst A.

TABLE 1

Results with Catalyst A

Adsorbed gas	Number of molecules of gas adsorbed (CO or CO_2) per g catalyst $\times 10^{-19}$	Number of molecules of desorbed gas per g catalyst $\times 10^{-19}$			
		CO	CO_2	CH_4	H_2O
CO	6.1	2.3	1.8	—	—
CO + H_2	6.2	3.0	0.2	2.2	0.5
H_2 + CO	6.2	2.8	0.1	3.0	[a]
CO with H_2 flow	6.2	1.0	—	5.1	5.0
CO_2	3.4	—	3.4	—	—

[a] Not measured.

exposed to CO pulses until no additional CO adsorption was detected. The catalyst temperature was then increased at a constant rate in the helium carrier gas.

(iii) The catalyst was saturated with CO in a flow of 25% H_2 and 75% He, and then the catalyst temperature was increased at a constant rate in the H_2–He flow. This experiment was similar to that carried out by McCarty *et al.* (*3*).

These three experiments were carried out on each of the catalysts for CO hydrogenation and are described below.

Catalyst A. Figure 6 shows the resulting desorption spectra for experiment (i), CO adsorption followed by H_2 adsorption. The surface, after being saturated with CO, could still adsorb a large amount of H_2. During programmed heating one-third of the adsorbed CO reacted to form methane in a broad peak with a peak temperature of 340°C. A H_2O peak was also observed to start at the same temperature as the methane but the H_2O had a higher peak temperature and continued to desorb to very high temperatures. The amount of water formed, which could only be measured approximately because of the high temperature peak, was only one-fourth the amount of methane. The CO_2 peak decreased significantly from that shown in Fig. 1 but the curve shapes for CO and CO_2 were similar to those in Fig. 1.

Reversing the order of adsorption (experiment (ii) resulted in half of the adsorbed CO reacting to methane but the desorption peaks looked the same as in Fig. 6. The number of molecules leaving the surface is summarized in Table 1.

Temperature programmed reaction spectra resulting from experiment (iii), the reaction of adsorbed CO with flowing H_2, are presented in Fig. 7. Eighty-two percent

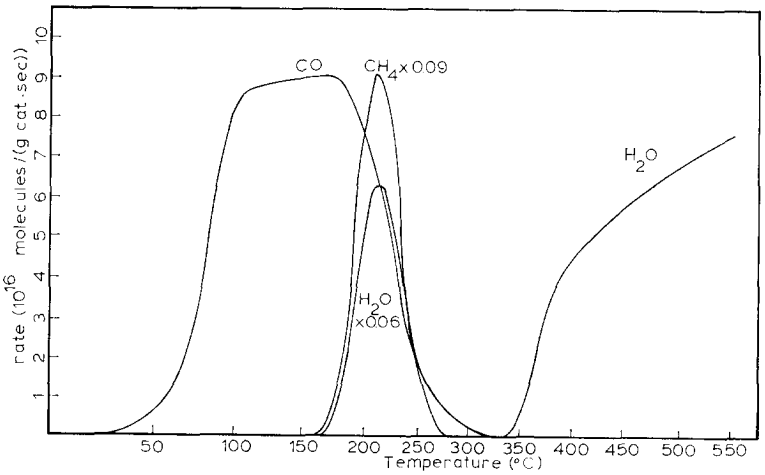

FIG. 7. CO, CH_4, and H_2O programmed reaction spectra (hydrogen flow) for CO adsorption on catalyst A.

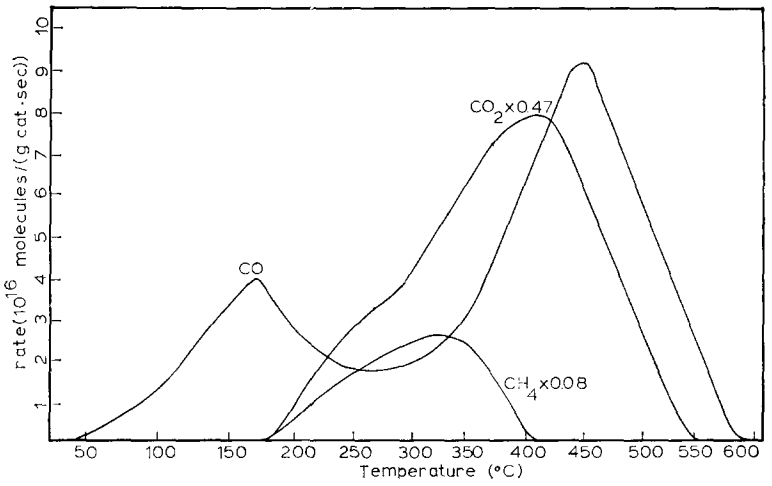

FIG. 8. CO, CH_4, CO_2 programmed reaction spectra for CO and H_2 coadsorption on catalyst B.

of the adsorbed CO reacted to methane in a narrow peak with a peak temperature of 225°C. A water peak with the same shape and peak temperature was also observed. However, an additional large water peak, starting near 350°C, was also observed. The water peak at 225°C and the methane peak each corresponded to 5.0×10^{19} molecules/g catalyst. The water peak above 350°C was even larger than this but no simultaneous CH_4 peak was observed. The low temperature CO peak was similar to that in Fig. 1 (although smaller), but, surprisingly, the higher temperature CO was completely absent. Also, *no* CO_2 desorption was detected.

Catalyst B. When CO and then H_2 were adsorbed on catalyst B, the yield to CH_4 was 40% during subsequent heating. The yield was slightly less for the reverse adsorption but the spectra were the same. The resulting spectra, shown in Fig. 8, were similar to CO/CO[1] and CO_2/CO but smaller, and the CH_4 desorbed in a broad group of peaks extending over the temperature range of 175 to 400°C. The water peak was not measured for this experiment.

The reaction of adsorbed CO with flowing H_2 resulted in a 91% conversion to CH_4. The methane was formed in a single peak with a peak temperature of 180°C as shown in Fig. 9. *No* CO_2 desorption was detected and the small CO desorption was complete by 250°C. A water peak was seen with the same peak temperature as the methane peak. However, in addition, a high temperature water peak, of much larger amplitude, was seen with a peak temperature of 460°C.

Catalyst C. Catalyst C was the least active catalyst for methanation; the yield to CH_4 was only 7% for CO and then H_2 coadsorption. The CO and CO_2 spectra, shown in Fig. 10, were very similar to CO/CO and CO_2/CO. The methane was formed with a peak temperature of 325°C. Water formed at essentially the same temperature, but only one-fourth the magnitude of the methane. For the reverse order of adsorption, *no* methane production was detected.

The methane product formed for reaction of adsorbed CO with flowing H_2 (see Fig. 11) was similar to that observed for catalysts A and B. Methane was formed

[1] A shorthand notation will be employed. For example, the notation A/B refers to desorbing gas A during a programmed heating following adsorption of gas B at room temperature.

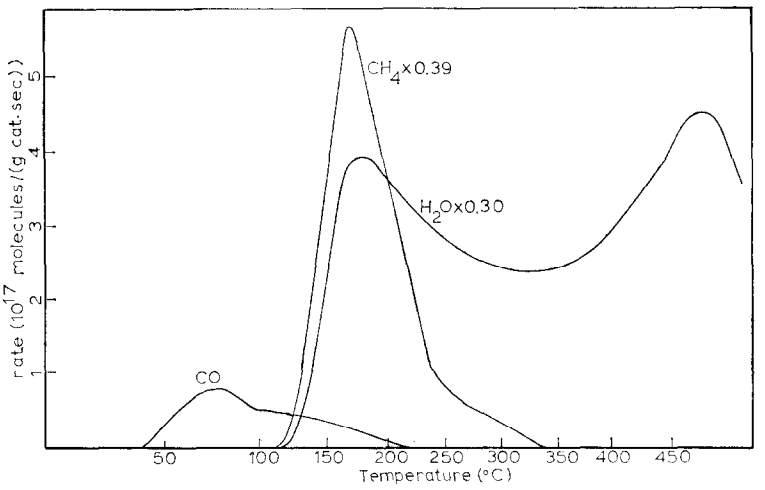

FIG. 9. CO, CH_4, and H_2O programmed reaction spectra (hydrogen flow) for CO adsorption on catalyst B.

with a 72% yield in a narrow peak with a peak temperature of 240°C; the CO desorption was complete by 275°C and no CO_2 desorption was observed. A water peak was seen with a peak temperature of 240°C and with an area corresponding to essentially the same number of molecules as in the CH_4 peak. However, the H_2O peak had a significant high temperature tail that persisted to 430°C.

Tables 2 and 3 summarize the results for catalysts B and C.

DISCUSSION

The CO desorption from the different catalysts will be compared to each other and to CO desorption from unsupported single crystals. The reaction studies will then be discussed with an aim to under-

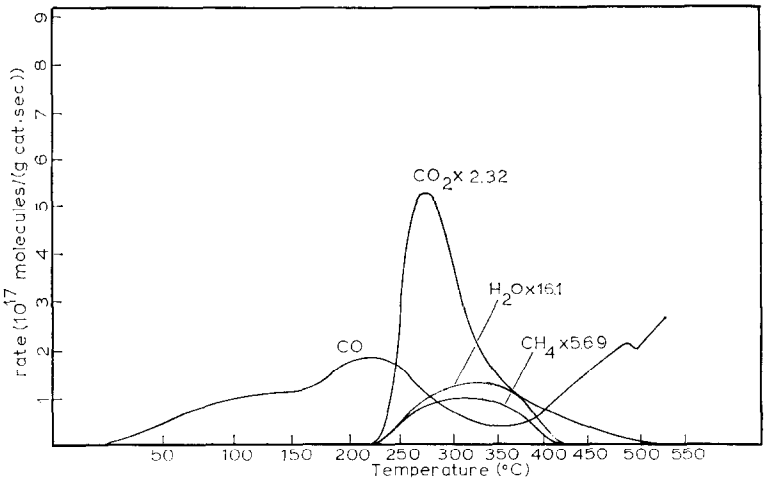

FIG. 10. CO, CO_2, and CH_4 programmed reaction spectra for CO and H_2 coadsorption on catalyst C.

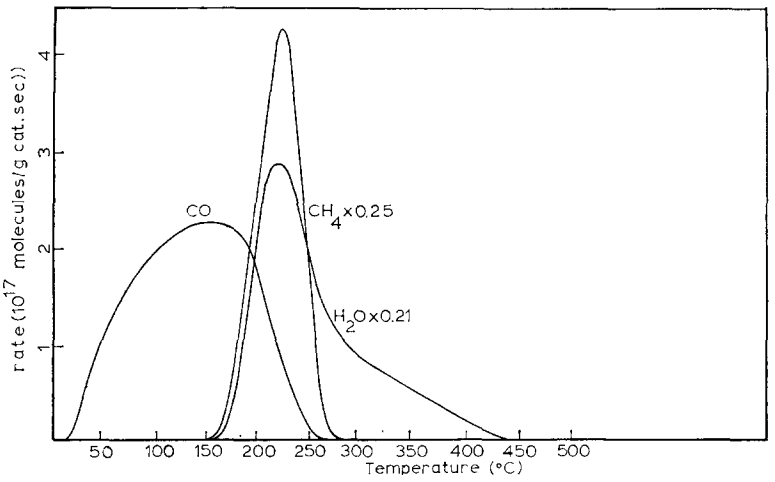

FIG. 11. CO, CH_4, and H_2O programmed reaction spectra (hydrogen flow) for CO adsorption on catalyst C.

stand better the mechanism and how the reactant adsorption properties relate to reaction properties.

Carbon Monoxide and Carbon Dioxide Desorption

On all three catalysts some of the adsorbed CO was very weakly bound, but the desorption curve shapes and peak temperatures were quite different on each of the catalysts. Only catalysts A and C exhibited CO desorption above 600°C. On all three catalysts more than half the adsorbed CO decomposed to yield CO_2 and surface carbon but the rates of decomposition (as indicated by the CO_2 peak temperatures), the CO_2 curve shapes and the amount of decomposition were different.

The three catalysts differ in their methods of preparation, in their supports, in their metal particle sizes, and in the additional materials, beside nickel, present on the support. A systematic study of the effect of particle size and support is needed to understand the cause of these differences.

For catalyst A the high temperature CO desorption may be due to the presence of the CaO and C in the catalyst and for catalyst C it may be due to components of

TABLE 2

Results with Catalyst B

Adsorbed gas	Number of molecules of gas adsorbed (CO or CO_2) per g catalyst $\times 10^{-19}$	Number of molecules of desorbed gas per g catalyst $\times 10^{-19}$			
		CO	CO_2	CH_4	H_2O
CO	8.3	2.2	3.1	—	—
CO + H_2	7.8	1.3	2.2	3.1	[a]
H_2 + CO	8.2	1.6	2.4	2.9	[a]
CO with H_2 flow	8.0	0.7	—	7.3	8.1
CO_2	3.4	—	3.4	—	—

[a] Not measured.

TABLE 3

Results with Catalyst C

Adsorbed gas	Number of molecules of gas adsorbed (CO or CO_2) per g catalyst $\times 10^{-19}$	Number of molecules of desorbed gas per g catalyst $\times 10^{-19}$			
		CO	CO_2	CH_4	H_2O
CO	7.9	1.8	3.1	—	—
CO + H_2	8.2	3.7	2.0	0.6	0.2
H_2 + CO	8.0	3.6	2.0	—	—
CO with H_2 flow	7.9	2.1	—	5.7	6.0

the kieselguhr. For both of these catalysts CO desorption at high temperature was observed without CO adsorption. For catalyst B the composition and preparation procedure are known, and no desorption of CO or CO_2 was observed above 600°C.

A comparison of the CO_2/CO peaks for each catalyst to the CO_2/CO_2 from that catalyst indicates that the CO_2/CO observed is from a reaction-limited and not desorption-limited step. It has been observed that CO_2 is formed during heating of a supported nickel catalyst in a carbon monoxide atmosphere (*9*) and that carbon forms on a surface following CO adsorption and heating (*10*). Also CH_4 formed in H_2 flow following CO_2 adsorption is different from CH_4 formed in H_2 flow following CO adsorption, implying CO_2 was not formed when CO was adsorbed but only as the CO_2 desorbed. Also, the data for CO_2 adsorption on the oxidized catalyst and the fact that CO_2 adsorption was significantly smaller on catalyst C indicate that most of the CO_2/CO_2 was coming from the alumina support. The fact that the CO_2/CO_2 desorptions were different for catalysts A and B may be due to the presence of CaO and C on catalyst A or to the differences in their alumina supports. Carbon dioxide adsorption has been observed on alumina (*11*, *12*) and the surface coverage reported by Morikawa and Amenomiya (*12*) was close to the surface coverage observed in the present experiments.

Thus on supported catalysts we can make several observations about CO adsorption. First, CO adsorption at room temperature appears to have several binding states, some of which have very high binding energies since CO desorption occurs at 500°C and higher. Second, during desorption a substantial fraction of the adsorbed CO reacts to form CO_2 and adsorbed carbon. Third, the binding states, the rate of reaction to CO_2, and the fraction of adsorbed CO converted to CO_2 are all functions of the catalyst preparation. Because CO adsorption on alumina is weak (*13*, *14*) it is not expected that these differences in catalysts are due to CO adsorption on the supports though it is possible a small amount of CO adsorption occurs on the supports and contributes to the low temperature peaks. Also, when CO adsorbs at room temperature it does not appear to dissociate to carbon and oxygen. Since the reaction in flowing H_2 indicates that both CH_4 and H_2O are formed at the same rate, the reaction is limited by C–O bond breaking. Thus the CO does not dissociate until elevated temperatures.

In contrast to CO desorption from supported nickel, the desorption of CO from single- and polycrystalline nickel has been extensively studied (*15–21*). Flash desorption in ultrahigh vacuum was used in several studies to determine the number of adsorbed states and the activation energies or binding energies of these states. Surprisingly, the surface coverages, the number of binding states, and the energies of these binding states were the same on several single crystal surfaces and on polycrystalline nickel (*15–21*). Most of the CO adsorbed in a single state with a binding energy of 30 to 32 kcal/mole. A smaller amount adsorbed in two other states with energies of 16 and 25 kcal/mole and these states were usually seen for adsorption below room temperature. It was also observed that when oxygen was adsorbed on a carbon-contaminated surface that two high temperature CO peaks were present, one at 375°C and one at 625°C (this peak was very broad) (*21*). Also, on none of these surfaces was CO_2 desorption observed; all the adsorbed CO desorbed as CO.

Likewise, CO_2 adsorption at room temperature has been studied on the Ni(110) and Ni(100) surfaces by flash desorption (*21*, *22*). No CO_2 desorption was detected for room temperature adsorption but CO desorption was observed similar to CO/CO desorption, and adsorbed oxygen was

observed on the surface by Auger spectroscopy.

A comparison of results for the supported and unsupported nickel shows that there is very little similarity between the two. On unsupported nickel CO desorption does not depend on the crystal face; on supported nickel it depends on catalyst preparation. On unsupported nickel all the adsorbed CO desorbs as CO; on supported nickel a large fraction reacts to CO_2. Only on a sputter-damaged Ni(111) surface was CO_2 desorption observed during heating following CO adsorption, and the CO decomposition was attributed to surface defects (*23*). It is likely the sputter-damaged surface more closely approximates the small particles on supported catalysts than the single crystal surfaces. On unsupported nickel all the CO desorption is essentially complete by 200°C for heating rates of 10°K sec^{-1}. On supported nickel CO desorption is observed at 500°C for heating rates of 1°K sec^{-1}. On unsupported nickel CO desorption above 200°C has been reported (*17*, *22*) when the CO covered surface was exposed to an electron beam before flashing. This high temperature CO was attributed to carbon–oxygen recombination. It certainly appears likely the high temperature CO seen here was also due to carbon–oxygen recombination. And finally, on unsupported nickel CO_2 adsorbs and decomposes during adsorption, while on supported nickel the adsorption is small and no decomposition was detected.

More experiments are needed to explain these large differences between the supported and unsupported nickel. However, the present experiments indicate that one must be careful in extrapolating data on unsupported macrocrystals to supported catalysts. Of course, the comparison above for supported and unsupported nickel was not made for the exact same experimental conditions and the observed differences may be due to differences between supported and unsupported nickel, to the large differences in pressures between the two type studies or to a combination of the two effects.

Coadsorption of CO and H_2

Each of the catalyst surfaces, though *saturated* with adsorbed CO, was able to adsorb a large amount of H_2 without desorbing any CO. Because of experimental difficulties the H_2 adsorption could not be accurately measured but the CH_4 formation could. For catalyst A, for example, the amount of CH_4 leaving the surface during heating required that 4.4×10^{19} molecules H_2/g catalyst were adsorbed on the surface. In addition, 0.5×10^{19} molecules of water were leaving the surface. Thus, *at least* 11.1×10^{19} molecules of CO plus H_2/g of catalyst were adsorbed on the surface simultaneously.

The coadsorption of CO and H_2 on nickel has been examined in several studies. Early studies [reviewed by Mills and Steffgen (*24*)] found that the preadsorption of a small amount of CO enhanced the quantity of H_2 subsequently adsorbed, while a large CO preadsorption inhibited H_2 adsorption. It was also found that treatment of chemisorbed CO with H_2 at room temperature shifted the ir band due to linear CO to a lower frequency and increased the relative amount of bridged CO.

The coadsorption of CO and H_2 has been recently studied on polycrystalline films by flash desorption (*20*). Though heating a nickel surface containing coadsorbed CO and H_2 yielded no methane product, it was seen that adsorbed H_2 caused an increase in the amount of CO adsorbed. It was also seen that at 273°K adsorbed H_2 was displaced by CO but adsorbed CO was not displaced by H_2.

Thus previous studies indicate that, as we have observed, a surface saturated with CO will still adsorb a large amount of H_2. Also, preadsorption of H_2 did not seem to

affect the amount of CO that would subsequently adsorb. The comparison of polycrystalline films to supported nickel still shows a discrepancy in that coadsorbed CO and H_2 did not react on the polycrystalline film but did react on the supported nickel. Also, the presence of adsorbed H_2 does not appear to change the CO binding energy to nickel (for example, compare the desorption spectra in Figs. 1 and 6).

The methane from coadsorption was formed over approximately the same broad temperature range on each of the catalysts. In each case methane started to form at the same temperature that carbon dioxide started to form. The amount of CO_2 formed was less in the presence than in the absence of coadsorbed hydrogen. On two of the catalysts (A and C) the carbon monoxide desorption peaks actually increased in the presence of coadsorbed hydrogen though the amount of adsorbed CO was not significantly different. On catalyst C the water product was formed at the same time as the methane though in a lesser quantity. The water from catalyst A started to form when CH_4 started but it continued to leave the surface up to high temperatures, well after all the methane was formed. The water peak was not recorded for catalyst B.

Temperature Programmed Reaction in Flowing H_2

McCarty *et al.* (*3*) have carried out the reaction of adsorbed CO with flowing H_2 on catalyst A using programmed heating, and we observed the same methane peak (i.e., same peak temperature and width) as they did, indicating reproducible behavior.

On catalyst A equal quantities of CH_4 and H_2O were formed at the same temperature with the same peak shape, indicating that the rates of formation of CH_4 and H_2O were limited by the same elementary reaction step. On catalysts B and C the water peak was also at the same temperature as the methane peak but the water had a much larger tail. On the two catalysts with alumina supports, A and B, water was observed up to very high temperatures and in very large quantities. The water coverage reported for catalyst A in Table 1 corresponds to the water peak at 220°C and it does not include water desorbing above 325°C. We have no explanation at present for the water observed at the higher temperatures.

If it is assumed a surface carbon is an intermediate in methanation, as proposed by Wentrcek *et al.* (*2*), McCarty *et al.* (*3*), and Araki and Ponec (*1*), then the rate-limiting step that forms CH_4 and H_2O simultaneously cannot be the reaction of the carbon with adsorbed hydrogen since it is highly unlikely that oxygen reacts with adsorbed hydrogen at the same rate. Rather, the rate-limiting step must be the splitting of the carbon–oxygen bond in carbon monoxide. The subsequent reactions with hydrogen are rapid. The absence of a hydrogen isotope effect for methanation on nickel has been recently reported by Dalla Betta and Shelef (*25*). This result led them to conclude that hydrogen was *not* involved in a rate-determining step, but rather the splitting of the C–O bond was the likely rate-determining step. Our results indeed confirm that this splitting of the CO bond is the rate-determining step in methanation of carbon monoxide. Palmer and Vroom (*26*) studied methanation of CO on foils at low temperature and concluded also that direct disproportionation of CO at the surface is the rate-determining step in methanation. Also, the results of McCarty *et al.* (*3*) show that carbon on the surface is more reactive than adsorbed CO, indicating that CO bond breaking is the rate-limiting step and once the bond breaking occurs the reaction of adsorbed carbon with hydrogen is rapid. This conclusion about the rate-determining step is contrary to that presented by

Joyner using information obtained from clean surface studies (*27*).

Comparison of the data in Tables 1–3 for the H_2 flow experiments indicates that within experimental accuracy, all the adsorbed carbon monoxide left the surface as CO or CH_4 and H_2O, so that no surface carbon remained. In the absence of H_2, some of the adsorbed carbon was left on the surface after heating. The reaction in the absence of H_2 must occur in the following steps:

$$CO(g) \rightleftarrows CO(a) \quad (1)$$

$$CO(a) \rightleftarrows C(a) + O(a) \quad (2)$$

$$CO(a) + O(a) \rightarrow CO_2(a) \quad (3)$$

$$CO_2(a) \rightarrow CO_2(g) \quad (4)$$

In the presence of sufficient hydrogen the reactions

$$H(a) + O(a) \rightarrow OH(a) \quad (5)$$

$$OH(a) + H(a) \rightarrow H_2O(a) \quad (6)$$

$$H_2O(a) \rightarrow H_2O(g) \quad (7)$$

$$H(a) + C(a) \rightarrow CH(a) \quad (8)$$

$$CH(a) + H(a) \rightarrow CH_2(a) \quad (9)$$

$$CH_2(a) + H(a) \rightarrow CH_3(a) \quad (10)$$

$$CH_3(a) + H(a) \rightarrow CH_4(a) \quad (11)$$

$$CH_4(a) \rightarrow CH_4(g) \quad (12)$$

must be rapid compared to reaction (3). Thus, if sufficient adsorbed hydrogen is present, as is evidently the case in the hydrogen flow experiments, no CO_2 is formed. Also, comparison of CO_2/CO curves on each of the catalysts to CH_4 formed in H_2 flow from adsorbed CO indicates the CH_4 starts forming at a lower temperature than CO_2/CO, confirming that reactions (*8*)–(*12*) are faster than reaction (*3*). Since CO_2/CO does not correspond to CO_2/CO_2 it seems likely the CO_2 formation is limited by step (3). However, in the coadsorption experiments there is not sufficient hydrogen present and CO_2 is formed as its rate of formation becomes comparable to that of CH_4. A number of studies have indicated that CH_4 formation is first order in H_2 pressure so the smaller rate in the coadsorption experiment would be expected.

The dissociative CO mechanism implies CO breaks up to C and O and the carbon reacts rapidly to methane. In the absence of H_2 some of the CO desorbs as CO at the higher temperatures. In the presence of hydrogen it does not. This implies that starting near 200°C reaction (2) occurs and there is then a competition between the two reactions

$$CO(a) + O(a) \rightarrow CO_2(a)$$

$$CO(a) \rightarrow CO(g)$$

When coadsorption experiments rather than H_2 flow experiments were carried out, the rates of the two reactions were comparable since insufficient hydrogen was available on the surface. Thus for hydrogen coadsorption both CO and CO_2 desorbed from the surface, and CO desorption was larger for two of the catalysts than in the absence of hydrogen since less oxygen was available to form CO_2 by reaction (3). In the coadsorption experiments much less H_2O is formed than CH_4; this implies the reaction of hydrogen atoms with oxygen is comparable to the reactions of CO with oxygen. That is, the coadsorption experiments indicate that at low hydrogen coverages reactions (3) and (5) are of the same order of magnitude. Thus the adsorbed C reacts to methane but the oxygen that is formed from the bond splitting can react to form CO_2 or H_2O.

The similarity of the results for each of the catalysts implies that the same mechanisms are operating on the three different catalysts and the major differences are differences in desorption rates of CO, which may be due to differences in the rates of the reactions $C(a) + O(a) \rightarrow CO(a)$ and $CO(a) + O(a) \rightarrow CO_2(a)$.

These experiments on three different catalysts indicate that the reaction to

methane does *not* appear to depend very much on the binding energy of CO to the nickel surface. That is, the methane peak has similar peak temperatures and half widths on each of the catalysts *but* the CO desorption spectra shown in Figs. 1, 3, and 5 are quite different on each of the catalysts.

CONCLUSIONS

On supported nickel catalysts the rate of methane formation from adsorbed carbon monoxide appears to be limited by the rate of breaking of the carbon–oxygen bond. Once this bond breaks, as long as sufficient hydrogen is present on the surface, methane and water form rapidly and are observed as a narrow peak in the temperature-programmed spectra. The results from this temperature programmed desorption and reaction study are thus consistent with the dissociative CO mechanism for methanation proposed by a number of authors.

Also, the desorption properties of adsorbed carbon monoxide are very dependent on the catalyst properties. Both the desorption of carbon monoxide and the rate of formation of carbon dioxide product were different on each of the three catalysts. Since these differences are easily detected, temperature programmed desorption appears to be a very effective method of characterizing supported metal catalysts.

ACKNOWLEDGMENTS

This material is based upon work supported by the National Science Foundation under Grant No. ENG 76-09223. Their support is gratefully acknowledged. We would like to thank Dr. James A. Schwarz and Chevron Research Corporation for donation of the mass spectrometer used in this research. Also, we are grateful to Professor Calvin A. Bartholomew, Girdler Chemical Inc., and Harshaw Chemical Co. for donations of catalyst samples.

REFERENCES

1. Araki, M., and Ponec, V., *J. Catal.* **44**, 439 (1976).
2. Wentrcek, P. R., Wood, B. J., and Wise, H., *J. Catal.* **43**, 363 (1976).
3. McCarty, J. G., Wentrcek, P. R., and Wise, H., Preprint, ACS Meeting, Chicago, August 1977.
4. Vannice, M. A., *J. Catal.* **40**, 129 (1975).
5. Vannice, M. A., *J. Catal.* **37**, 462 (1975).
6. Falconer, J. L., and Wise, H., *J. Catal.* **43**, 220 (1976).
7. Bartholomew, C. H., and Farrauto, R. J., *J. Catal.* **45**, 41 (1976).
8. Bartholomew, C. H., private communication, 1977.
9. Heal, M. J., Leisegang, E. C., and Torrington, R. G., *J. Catal.* **42**, 10 (1976).
10. Van Dyk, W. L., Groenewegen, J. A., and Ponec, V., *J. Catal.* **42**, 10 (1976).
11. Amenomiya, Y., Morikawa, Y., and Pleizier, G., *J. Catal.* **46**, 431 (1977).
12. Morikawa, Y., and Amenomiya, Y., *J. Catal.* **48**, 120 (1977).
13. Della Gatta, G., Fubeni, B., Ghiotti, G., and Mortena, C., *J. Catal.* **43**, 90 (1976).
14. Scholten, J. J. F., and VanMontfoort, A., *J. Catal.* **1**, 85 (1962).
15. Falconer, J. L., and Madix, R. J., *Surface Sci.* **48**, 393 (1975).
16. Taylor, T. N., and Estrup, P. J., *J. Vacuum Sci. Tech.* **10**, 26 (1973).
17. Madden, H. H., and Ertl, G., *Surface Sci.* **35**, 211 (1973).
18. Tracy, J. C., *J. Chem. Phys.* **56**, 2736 (1972).
19. Conrad, H., Ertle, B., Kuppers, J., and Latta, I. E., *Surface Sci.* **57**, 475 (1976).
20. Wedler, G., Papp, H., and Schrool, G., *Surface Sci.* **44**, 463 1974).
21. Benziger, J. B., Madix, R. J., Aldag, A. W., and Lee, C. O., to be published.
22. McCarty, J., Falconer, J., and Madix, R. J., *J. Catal.* **30**, 235 (1973).
23. Eastman, D. E., Demuth, J. E., and Baker, J. M., *J. Vac. Sci. Tech.* **11**, 273 (1974).
24. Mills, G. A., and Steffgen, F. W., *Catal. Rev.* **8**, 159 (1973).
25. Della Betta, R. A., and Shelef, M., *J. Catal.* **49**, 383 (1977).
26. Palmer, R. L., and Vroom, D. A., *J. Catal.* **50**, 248 (1977).
27. Joyner, R. W., *J. Catal.* **50**, 176 (1977).